On a multiple time-scales perturbation analysis of a Stefan problem with a time-dependent Dirichlet boundary condition

Ihsan, A. F.; van Horssen, W. T.; Tuwankotta, J. M.

DOI
10.1016/j.nonrwa.2023.103961

Publication date
2024

Document Version
Final published version

Published in
Nonlinear Analysis: Real World Applications

Nonlinear Analysis: Real World Applications 75 (2024) 103961

Contents lists available at ScienceDirect

Nonlinear Analysis: Real World Applications

www.elsevier.com/locate/nonrwa

On a multiple time-scales perturbation analysis of a Stefan problem with a time-dependent Dirichlet boundary condition

A.F. Ihsan [a], W.T. van Horssen [b], J.M. Tuwankotta [a,*]

[a] *Analysis and Geometry, Faculty of Mathematics and Natural Sciences, Institut Teknologi Bandung, Indonesia*
[b] *Delft Institute of Applied Mathematics, Delft University of Technology, Netherlands*

A R T I C L E I N F O

Article history:
Received 28 October 2022
Accepted 10 July 2023
Available online xxxx

Keywords:
Multiple time-scales
Stefan problem
Time-dependent boundary temperature

A B S T R A C T

In this paper, a classical Stefan problem with a prescribed and small time-dependent temperature at the boundary is studied. By using a multiple time-scales perturbation method, it is shown analytically how the moving boundary profile is influenced by the prescribed temperature at the boundary and the initial conditions. Only a few exact solutions are available for this type of problems and it turns out that the constructed approximations agree very well with these exact solutions. In particular, approximations of solutions for this type of problems, with periodic and decaying temperatures at the boundary, are constructed. Furthermore, these approximations are valid on a long time scale, and seems to be not available in the literature.

1. Introduction

The classical Stefan problem was introduced with the aim on describing the evolution of the boundary (or interface) between two phases, i.e. the liquid and solid phase in ice melting. Also known as moving boundary problem, it has been studied for more than a century. Since its introduction, a large number of applications of Stefan problem can be found in the literature, such as solidification of a liquid [1], melting of an ice sheet with heat convection in the liquid phase [2,3], mushy area formation between two phases [4], three-phase transition models [5], diffusion or dissolution of particles [6–8], and many more. For a more comprehensive review of the existing applications, the reader is referred to the classical books [9,10].

The existence and uniqueness of solution for such problems can be found in the literature, see [11,12]. However, exact analytical solutions are only available for some very specific cases. Furthermore, most Stefan problems are solved approximately by means of numerical methods (see for instance [6–8,13–18]). Another alternative to approximate the solution is by using a straightforward naive perturbation expansion (see for

* Corresponding author.
E-mail address: jmtuwankotta@itb.ac.id (J.M. Tuwankotta).

https://doi.org/10.1016/j.nonrwa.2023.103961

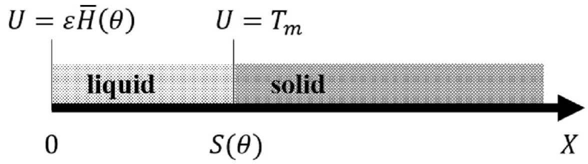

Fig. 1. Melting process of a semi-infinite ice sheet due to the temperature $\varepsilon\bar{H}(\theta)$ at $X = 0$.

instance [6,7,19–25]). There are a number of drawbacks for this approach. Firstly, this approximation is only valid on a rather short time-scale. Secondly, this approximation is constructed from a stationary solution, which implies that only very specific boundary and initial conditions can be considered.

In this paper, we consider a Stefan problem which is similar to the one studied in [19,26]. At the fixed boundary, instead of considering a time-dependent heat flux as is in [23,26], in this paper we consider a time-dependent temperature profile. We present the formulation of the problem in Section 2 of this paper. Rather than using straightforward expansions, a two time-scales perturbation method is applied to our problem in Section 3 of this paper. Various examples on how this method is applied to different kind of problems can be found in standard books on perturbation methods, e.g. [27–29]. By using this method, accurate approximations of the solutions of the classical Stefan problem subject to a constant temperature at the fixed boundary, are constructed and compared with exact solutions in Section 4. We show that the constructed approximation agrees very well with the exact solution on long time-scales. In Section 5 of this paper, time-dependent boundary conditions, such as a periodic temperature or a decaying temperature at the fixed endpoint, are introduced. Furthermore, accurate approximations for the solutions of these problems on long time-scales are constructed. To our knowledge, these results are new in the literature. Finally, in Section 6 of this paper, we draw some conclusions.

2. Formulation of the problem

Consider a one-dimensional Stefan problem with a Dirichlet boundary condition at the fixed endpoint:

$$\rho c \partial_\theta T(X,\theta) = K\partial_X^2 T(X,\theta), \quad 0 < X < S(\theta), \quad \theta > 0, \tag{1a}$$

$$-K\partial_X T(S(\theta),\theta) = \rho L S'(\theta), \tag{1b}$$

$$T(S(\theta),\theta) = T_m, T(0,\theta) = \varepsilon\bar{H}(\theta), \tag{1c}$$

$$T(X,0) = T_m + \varepsilon\bar{F}(X), \quad 0 < X < S(0) = b. \tag{1d}$$

This problem describes an ice melting problem (see also [26]). In this problem, $T(X,\theta)$ represents the temperature of the liquid phase at location X and time θ. The parameters ρ, c, K, L, and T_m represent the density, the heat capacity, the heat conductivity, the latent heat, and the freezing temperature of the water, respectively. The function $S(\theta)$ describes the moving interface position between the water and the ice.

The incoming heat that melts the ice is provided by a given time-dependent, positively definite function $\varepsilon\bar{H}(\theta)$, where ε is a small parameter. The initial location of the interface is given by the positive constant b, so that it is assumed that the liquid phase already exists initially. And the function $\bar{F}(x)$ is the x-dependent part of the initial temperature distribution. See Fig. 1 for an illustration for the problem we are considering.

Let us introduce the following scaling transformations:

$$\tau = \frac{K}{c\rho}\theta, \quad U(X,\tau) = \frac{c}{L}\left(T(X,\theta) - T_m\right),$$

$$F(X) = \frac{c}{L}(\bar{F}(X) - T_m), \quad \text{and} \quad H(\tau) = \frac{c}{L}\bar{H}(\theta),$$

so that problem (1a)–(1d) can be reformulated in the following non-dimensional form:

$$\partial_\tau U(X,\tau) = \partial_{XX}U(X,\tau), \qquad 0 < X < S(\tau), \quad \tau > 0, \tag{2a}$$
$$-\partial_X U(S(\tau),\tau) = S'(\tau), \qquad \tau \geq 0, \tag{2b}$$
$$U(S(\tau),\tau) = 0, \qquad \tau \geq 0, \tag{2c}$$
$$U(0,\tau) = \varepsilon H(\tau) \qquad \tau \geq 0, \tag{2d}$$
$$U(X,0) = \varepsilon F(X), \qquad 0 < X < S(0) = b, \tag{2e}$$

where H and F are positive-definite functions. The notations ∂_η for a partial derivative $\frac{\partial}{\partial \eta}$, and $'$ for a derivative of a one-variable function, are used throughout the paper. To immobilize the moving boundary, we define:

$$t(\tau) = \int_0^\tau S^{-2}(\eta)d\eta, \quad x = \frac{X}{s(t)}, \quad \text{and} \quad v(x,t) = U(X,\tau).$$

Substituting the transformation into the problem (2a)–(2e), the following equations for $v(x,t)$ are obtained:

$$-\partial_x v(x,t)\frac{x}{s(t)}s'(t) + \partial_t v(x,t) = \partial_{xx}v(x,t), \qquad 0 < x < 1, \qquad t \geq 0, \tag{3a}$$
$$v(0,t) = \varepsilon h(t), \qquad t \geq 0 \tag{3b}$$
$$\partial_x v(1,t) = -\frac{1}{s(t)}s'(t), \qquad t \geq 0, \tag{3c}$$
$$v(1,t) = 0, \qquad t \geq 0, \tag{3d}$$
$$v(x,0) = \varepsilon f(x), \qquad 0 < x < 1, \tag{3e}$$

where $f(x) = F(X)$, $s(t) = S(\tau)$, and $h(t) = H(\tau)$. Next, we remove the dependence on $s(t)$ in (3a) by substituting (3c) into (3a), i.e.,

$$\partial_t v(x,t) = \partial_{xx}v(x,t) - x\partial_x v(x,t)\partial_x v(1,t).$$

Finally, the following rescaling, $v = \varepsilon u$, is introduced since small initial and boundary conditions are considered. Problem (3a)–(3e) then becomes:

$$\partial_t u(x,t) = \partial_{xx}u(x,t) - \varepsilon x\partial_x u(x,t)\,\partial_x u(1,t), \qquad 0 < x < 1, \quad t \geq 0, \tag{4a}$$
$$u(0,t) = h(t), \qquad t \geq 0, \tag{4b}$$
$$u(1,t) = 0, \qquad t \geq 0, \tag{4c}$$
$$u(x,0) = f(x), \qquad 0 < x < 1. \tag{4d}$$

System (4a)–(4d) consists of a weakly nonlinear diffusion equation subject to an initial condition and subject to linear Dirichlet boundary conditions on a fixed spatial domain.

3. The two time-scales perturbation method

When applying a straightforward perturbation expansion for $u(x,t)$ in (4a)–(4d), one usually encounters terms in the equation which produce unbounded solution. These terms are usually called secular terms. To avoid these secular terms and to obtain approximations which are valid on long time-scales, a two time-scales perturbation method will be used to (approximately) solve problem (4a)–(4d). It is assumed that the solution depends on $t_0 = t$ and $t_1 = \varepsilon t$, and that $u(x,t)$ can be expanded as

$$u(x,t) = u_0(x,t_0,t_1) + \varepsilon u_1(x,t_0,t_1) + \mathcal{O}(\varepsilon^2).$$

By applying the time derivative operator: $\partial_t = \partial_{t_0} + \varepsilon \partial_{t_1}$, and by replacing u in (4a)–(4d) by its expansion, and then by collecting terms of equal order in ε, we obtain a family of initial–boundary value problems for u_0, u_1, u_2, and so on. For our purpose, let us look at the problems for u_0 and u_1 only, i.e.:

$$\mathcal{O}(1): \quad \partial_{t_0} u_0(x,t_0,t_1) - \partial_{xx} u_0(x,t_0,t_1) = 0 \tag{5a}$$

$$u_0(0,t_0,t_1) = h(t_0), \tag{5b}$$

$$u_0(1,t_0,t_1) = 0, \tag{5c}$$

$$u_0(x,0,0) = f(x), \tag{5d}$$

$$\mathcal{O}(\varepsilon): \quad \partial_{t_0} u_1(x,t_0,t_1) - \partial_{xx} u_1(x,t_0,t_1) = -\partial_{t_1} u_0(x,t_0,t_1) - x\partial_x u_0(x,t_0,t_1)\partial_x u_0(1,t_0,t_1), \tag{5e}$$

$$u_1(0,t_0,t_1) = 0, \tag{5f}$$

$$u_1(1,t_0,t_1) = 0, \tag{5g}$$

$$u_1(x,0,0) = 0. \tag{5h}$$

By solving (5a)–(5d), and (5e)–(5d), we construct an $\mathcal{O}(\varepsilon)$ approximation for the solution on a time-scale of order $\frac{1}{\varepsilon}$.

$\mathcal{O}(1)$-Part of the problem

To solve the $\mathcal{O}(1)$ problem, let us introduce another transformation

$$\tilde{u}_0(x,t_0,t_1) = u_0(x,t_0,t_1) - h(t_0)(1-x).$$

Substituting this to (5a)–(5d), we obtain

$$\begin{aligned} \partial_{t_0}\tilde{u}_0 &= \partial_{xx}\tilde{u}_0 + H_0(x,t_0), \\ \tilde{u}_0(0,t_0,t_1) &= \tilde{u}_0(1,t_0,t_1) = 0, \\ \tilde{u}_0(x,0,0) &= f(x) - h(0)(1-x), \end{aligned}$$

where $H_0(x,t_0) = -h'(t_0)(1-x)$. Suppose that the non-homogeneous solution can be written as

$$\tilde{u}_0(x,t_0,t_1) = \sum_{n=1}^{\infty} u_{0n}(t_0,t_1)\phi_n(x),$$

where $\phi_n(x) = \sin(n\pi x)$. Substituting this into Eq. (5a) yields

$$\partial_{t_0} u_{0m}(t_0,t_1) + (m\pi)^2 u_{0m}(t_0,t_1) = 2\int_0^1 H_0(x,t_0)\phi_m(x)dx.$$

For convenience, we present the integral in the right-hand side of the equation as a Fourier series, yielding

$$H_{0n}(t_0) = 2\int_0^1 -h'(t_0)(1-x)\sin(n\pi x)dx = -\frac{2h'(t_0)}{n\pi}.$$

Using the method of integrating factors, we can solve the ODE for u_{0n}, i.e.,

$$u_{0n}(t_0,t_1) = C_{0n}(t_1)e^{-(n\pi)^2 t_0} - \frac{2}{n\pi}\int_0^{t_0} e^{(n\pi)^2(\eta - t_0)} h'(\eta)d\eta. \tag{6}$$

The general solution for the $\mathcal{O}(1)$ problem is

$$u_0(x,t_0,t_1) = \sum_{n=1}^{\infty} u_{0n}(t_0,t_1)\sin(n\pi x) + h(t_0)(1-x).$$

Moreover, using the initial condition, we obtain

$$C_{0n}(0) = 2\int_0^1 [f(x) - h(0)(1-x)]\phi_n(x)dx = f_n - \frac{2h(0)}{n\pi}, \tag{7}$$

where f_n is the nth Fourier series coefficient of $f(x)$. Note that for each n, the solution in (6) still depends on an unknown function $C_{0n}(t_1)$. We will solve the $\mathcal{O}(\varepsilon)$ part of the problem to determine this function.

$\mathcal{O}(\varepsilon)$-Part of the problem

To solve (5e)–(5h), let us denote

$$H_1(x,t_0,t_1) = -\partial_{t_1}u_0(x,t_0,t_1) - x\partial_x u_0(x,t_0,t_1)\partial_x u_0(1,t_0,t_1).$$

Substituting u_0 into H_1 gives:

$$\begin{aligned} H_1(x,t_0,t_1) = \sum_{n=1}^{\infty}\partial_{t_1}u_{0n}(t_0,t_1)\phi_n(x) - x\Bigg[&h^2(t_0) - h(t_0)\sum_{n=1}^{\infty}u_{0n}(t_0,t_1)(\phi_n'(1)+\phi_n'(x)) \\ &+\sum_{n=1}^{\infty}\sum_{m=1}^{\infty}u_{0n}(t_0,t_1)u_{0m}(t_0,t_1)\phi_n'(x)\phi_m'(1)\Bigg]. \end{aligned}$$

With a similar procedure as is done previously, we write

$$u_1(x,t_0,t_1) = \sum_{n=1}^{\infty}[u_{1n}(t_0,t_1)\sin(n\pi x)], \tag{8}$$

where

$$u_{1n}(t_0,t_1) = e^{-(n\pi)^2 t_0}\left[C_{1n}(t_1) + \int_0^{t_0} e^{(n\pi)^2\eta}H_{1n}(\eta,t_1)d\eta\right], \quad \text{and} \tag{9}$$

$$H_{1n}(t_0,t_1) = \frac{\langle H_1,\phi_n\rangle}{\langle \phi_n,\phi_n\rangle}. \tag{10}$$

and $\langle \_,\_\rangle$ is an inner product in $L_2[0,1]$ as vector space over $\mathbb{R}$, i.e. $\langle f,g\rangle = \int_0^1 f(x)g(x)dx$. By using the initial conditions, we obtain $C_{1n}(0) = 0$. We then can compute H_{1n} as follows.

$$\begin{aligned} H_{1n}(t_0,t_1) = &-u_{0nt_1}(t_0,t_1) + \frac{3h(t_0)u_{0n}(t_0,t_1)}{2} \\ &- \frac{2h^2(t_0)(-1)^{n+1}}{\pi n} + 2h(t_0)\sum_{m\neq n}u_{0m}(t_0,t_1)(1-K_{mn}) \\ &- 2\sum_{p=1}^{\infty}u_{0p}(t_0,t_1)\phi_p'(1)\left(\frac{u_{0n}(t_0,t_1)}{4} + \sum_{m\neq n}u_{0m}(t_0,t_1)K_{mn}\right), \end{aligned}$$

where $K_{mn} = -\frac{(2n-1)^2(-1)^{m+n}}{(m+n-1)(m-n)}$. In order to completely compute u_{1n}, we need an explicit expression for $h(t)$. In Section 4 and in Section 5 of this paper, we will determine u_{0n} and u_{1n} for various choices of $h(t)$.

Moving boundary profile

To obtain the moving boundary profile, we use the boundary condition (3c), that is, $\partial_x v(1,t) = -\frac{s'(t)}{s(t)}$, which in fact is an ODE for $s(t)$. Using the initial condition $s(0) = b$, the ODE can be solved directly, yielding

$$\begin{aligned} s(t) &= b\exp\left(-\int_0^t \partial_x v(1,\eta)d\eta\right) \\ &= b\exp\left[-\varepsilon\int_0^t \left[\sum_{n=1}^{\infty}\left(C_{0n}(\varepsilon\theta)e^{-(n\pi)^2\theta}\right.\right.\right. \\ &\left.\left.\left.+\frac{2}{n\pi}\int_0^\theta e^{(n\pi)^2(\eta-\theta)}h'(\eta)d\eta\right)n\pi(-1)^n - h(\theta)\right]d\theta + \mathcal{O}(\varepsilon^2)\right]. \end{aligned} \tag{11}$$

To determine s completely, we need to obtain the unknown function C_{0n}. In the following sections, we will compute C_{0n} and so $s(t)$ for specific choices for the function $h(t)$.

4. The case with a constant temperature at the boundary: $h(t) = a$

4.1. Removing secular terms

Suppose $h(t) = a$, where a is a positive constant, then u_{0n} easily follows from (6):

$$u_{0n}(t_0,t_1) = C_{0n}(t_1)e^{-(n\pi)^2 t_0},$$

and the $\mathcal{O}(1)$ solution becomes

$$u_0(x,t_0,t_1) = \sum_{n=1}^{\infty} C_{0n}(t_1)e^{-(n\pi)^2 t_0}\sin(n\pi x) + a(1-x). \tag{12}$$

The function $C_{0n}(t_1)$ still has to be determined, and follows from (9) by demanding that u_{1n} is bounded, or equivalently, by removing secular terms in u_{1n}. From Eq. (9), we see that the formula for the order $\mathcal{O}(\varepsilon)$ solution contains an integral. To simplify the notation, we introduce

$$L_{nmp}(t_0) = \frac{e^{\left[n^2-m^2-p^2\right]\pi^2 t_0} - 1}{(n^2-m^2-p^2)\pi^2}, \quad L_{nm}(t_0) = L_{nm0}(t_0), \quad L_n(t_0) = L_{n00}(t_0). \tag{13}$$

Then,

$$\begin{aligned} &\int_0^t e^{(n\pi)^2\eta}H_{1n}(\eta,t_1)d\eta \\ &= t_0\left(-C_{0n}' + \frac{3aC_{0n}}{2} - 2\sum_{p\neq n} p\pi(-1)^p C_{0\sqrt{n^2-p^2}}C_{0p}K_{\sqrt{n^2-p^2}n}\right) \\ &\quad - \frac{2a^2(-1)^{n+1}L_n}{\pi n} + \sum_{m\neq n} 2aC_{0m}L_{mn}(1-K_{mn}) \\ &\quad - 2\sum_{p=1}^{\infty}\phi_p'(1)\left(\frac{C_{0p}C_{0n}L_{nnp}}{4} + \sum_{\substack{m\neq n\\ m^2\neq n^2-p^2}} C_{0m}C_{0p}L_{nmp}K_{mn}\right). \end{aligned} \tag{14}$$

The terms inside the first brackets, which are multiplied by t_0, are secular terms. To keep the solution bounded, we set

$$C'_{0n}(t_1) - \frac{3aC_{0n}(t_1)}{2} = W_n(t_1), \tag{15}$$

where

$$W_n(t_1) = -2\sum_{p\neq n} p\pi(-1)^p C_{0\sqrt{n^2-p^2}} C_{0p} K_{\sqrt{n^2-p^2}n}.$$

Observe that W_n is nonzero only for some values of n. We can see this by the fact that W_n is a sum over p which satisfies the Pythagorean formula $n^2 = m^2 + p^2$ with $n, m, p \in \mathbf{N}^+$. For example, in case of n less than 5, there is no p which satisfies the Pythagorean formula, so W_n is zero for n less than 5.

4.2. On the Pythagorean triple

The term $W_n(t_1)$ in Eq. (15) is coupled to other equations for C_{0m}. To be precise, for each value of n, the differential Eq. (15) depends on other equations with index j and k where (j, k, n) is a Pythagorean triple. For example, the following is a list of Pythagorean triples (j, k, n) corresponding to values of n up to 20.

- $(3, 4, 5)$
- $(6, 8, 10)$
- $(5, 12, 13)$
- $(9, 12, 15)$
- $(8, 15, 17)$
- $(12, 16, 20)$

If n does not correspond to a triple, then $W_n(t_1)$ vanishes, and Eq. (15) reduces to

$$C'_{0n} - \frac{3aC_{0n}}{2} = 0,$$

which has the following solution

$$C_{0n}(t_1) = C_{0n}(0)e^{\frac{3at_1}{2}}, \tag{16}$$

where the initial condition $C_{0n}(0)$ is given in (7). However, if (j, k, n) is a Pythagorean triple for some integers j and k, $W_n(t_1)$ becomes

$$W_n(t_1) = \frac{2\pi n^3}{jk} C_{0j}(t_1)C_{0k}(t_1).$$

In some cases, one value of n may correspond to more than one triple. In that case, $W_n(t_1)$ contains more terms. An example of this is $n = 25$, i.e. $(15, 20, 25)$ and $(7, 24, 25)$. For this case, we write

$$W_n(t_1) = \sum_{(j,k,n)\in P_n} q_{jkn}(t_1), \qquad q_{jkn}(t_1) = \frac{2\pi n^3}{jk} C_{0j}(t_1)C_{0k}(t_1),$$

where P_n is the set of all Pythagorean triples corresponding to n. Actually, for most values of n, one finds only one isolated triple, at least for values up to $n = 300$. Formally, one can rewrite Eq. (15) into the following equivalent integral equation:

$$C_{0n}(t_1) = e^{\frac{3at_1}{2}} \left[C_{0n}(0) + \int_0^{t_1} W_n(\eta)e^{-\frac{3a\eta}{2}} d\eta \right]. \tag{17}$$

If neither j nor k is a hypotenuse of another Pythagorean triple, then C_{0j} and C_{0k} are given by (16) for $n = j$ and $n = k$, respectively. And so, $q_{jkn}(t_1)$ becomes:

$$q_{jkn}(t_1) = \frac{2\pi n^3}{jk} C_{0j}(0)C_{0k}(0)e^{3at_1}.$$

Thus, the integral in (17) can be computed easily, and one obtains

$$C_{0n}(t_1) = e^{\frac{3at_1}{2}} \left[C_{0n}(0) + \left(e^{\frac{3at_1}{2}} - 1 \right) \sum_{(j,k,n)\in P_n} \frac{4\pi n^3}{3ajk} C_{0j}(0) C_{0k}(0) \right]. \tag{18}$$

Otherwise, if j or k is a hypotenuse in another triple, then the solution for C_{0j} or C_{0k} is in the form of (18). An example for this is the triple $(5,12,13)$, where 5 is a hypotenuse for the triple $(3,4,5)$. Let for example, k correspond to a triple (k_1,k_2,k), then q_{jkn} becomes

$$q_{jkn}(t_1) = \frac{2\pi n^3}{jk} e^{3at_1} C_{0j}(0) \left[C_{0k}(0) + \left(e^{\frac{3at_1}{2}} - 1 \right) \sum_{(k_1,k_2,k)\in P_k} \frac{4\pi k^3}{3ak_1k_2} C_{0k_1}(0) C_{0k_2}(0) \right].$$

The solution for C_{0n} in this case becomes

$$\begin{aligned} C_{0n}(t_1) = e^{\frac{3at_1}{2}} \Bigg[& C_{0n}(0) + \left(e^{\frac{3at_1}{2}} - 1 \right) \sum_{(j,k,n)\in P_n} \frac{4\pi n^3}{3ajk} C_{0j}(0) C_{0k}(0) \\ & + \frac{2\pi n^3}{3ajk} \left(e^{3at_1} - 2e^{\frac{3at_1}{2}} \right) \sum_{(k_1,k_2,k)\in P_k} \frac{4\pi k^3}{3ak_1k_2} C_{0k_1}(0) C_{0k_2}(0) \Bigg]. \end{aligned} \tag{19}$$

The complexity of the solution may not stop here. In the last computation, we assume that only one leg, i.e. k, corresponds to another triple. In some cases though, this chain of triples may be more complex and longer.

Let us define some terminology. We define a *Pythagorean chain* as a tuple (ordered set) of numbers such that (i) each member of the tuple is a hypotenuse of a Pythagorean triple; (ii) each but one member of the tuple must also be a leg of another member's triple. We will write the tuple with square brackets to avoid confusion with the triples. The only member that is not a leg of another triple is called *head*. We also define the *length of the chain* as the number of chain members. For example, as we have seen before, we have $[13,5]$ as a Pythagorean chain of length-2. Another example is $[17,15]$ which forms a chain because there are triples $(8,15,17)$ and $(9,12,15)$. If a chain has length-1, then we call it an *isolated triple*.

In Eq. (19), we describe the solution for the case when n is a head of a length-2 Pythagorean chain. Unfortunately, we may have longer chains for some values of n, which will add more terms in the solution.

For example, the case $n = 25$, which corresponds to the triple $(15,20,25)$, is a case for which each leg corresponds to a different triple, i.e., $(12,16,20)$ and $(9,12,15)$. This example forms a length-3 chain $[25,20,15]$. A longer chain of triples may also occur.

Now take a look at the triple $(39,52,65)$. Leg 39 corresponds to $(15,36,39)$ and leg 52 corresponds to $(20,48,52)$. As we have seen in the previous example, number 15 and 20 itself are hypotenusa for other triples. This example shows a length-5 chain $[65,39,52,15,20]$. An illustration of this chain is shown in Fig. 2.

Interestingly, by counting systematically all triples with a hypotenuse up to 100, we obtain that there are 14 isolated triples, 20 chains of length-2, 4 chains of length-3, 1 chain of length-4, 2 chains of length-5, and 1 chain of length-6. By this observation, it is difficult to find a general form for the solution as the triples may branch off and form different chains. For the sake of simplicity, we just have to rewrite (19) as follows

$$C_{0n}(t_1) = e^{\frac{3at_1}{2}} \left[C_{0n}(0) + \left(e^{\frac{3at_1}{2}} - 1 \right) \sum_{(j,k,n)\in P_n} \frac{4\pi n^3}{3ajk} C_{0j}(0) C_{0k}(0) \right] + \cdots,$$

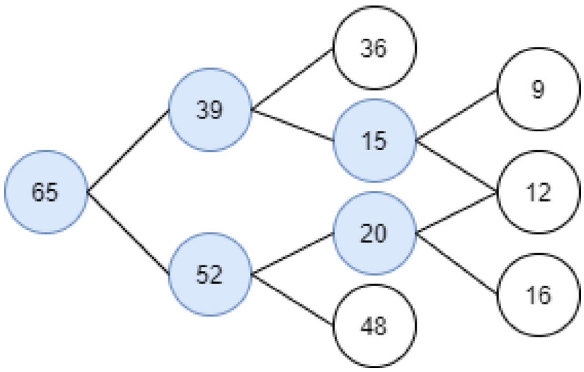

Fig. 2. Illustration of Pythagorean branching that occurs for the case with $n = 65$ as head of the chain.

so that it is similar to the basic form (18), where the dots represent the possibility for more terms due to the formation of chains. Thus, we can describe the "general" solution of (15) as

$$C_{0n}(t_1) = C_{0n}(0)e^{\frac{3at_1}{2}} + \begin{cases} C_{0j}(0)C_{0k}(0)\frac{4\pi n^3}{3ajk}\left(e^{3at_1} - e^{\frac{3at_1}{2}}\right) + \cdots, & \text{if there is at least one triple } (j,k,n), \\ 0, & \text{otherwise.} \end{cases} \tag{20}$$

4.3. Truncation method

Since we cannot construct the general form of the solution C_{0n}, it is also not possible to obtain an exact expression for the solution v, or for s. Alternatively, we can take only the first N-terms in the expansion of the solution. This truncation can be validated by arguing that the factors $e^{-(n\pi)^2 t_0}$ are exponentially small for all fixed $t_0 > 0$, and for n large. Thus, we consider the solution in the form:

$$u(x,t_0,t_1) = \sum_{n=1}^{N} C_{0n}(t_1)e^{-(n\pi)^2 t_0}\sin(n\pi x) + h(t_0)(1-x) + \mathcal{O}(\varepsilon).$$

It can also be shown that the first N-terms in the expansion for the solution give accurate approximations for $t = \mathcal{O}(\varepsilon^{-1})$. For simplicity, we choose $N = 4$ so that no Pythagorean triple occurs. In this case, we obtain immediately that

$$u(x,t_0,t_1) = \sum_{n=1}^{4}\left(f_n - \frac{2a}{n\pi}\right)e^{\frac{3at_1}{2} - (n\pi)^2 t_0}\sin(n\pi x) + a(1-x) + \mathcal{O}(\varepsilon). \tag{21}$$

For the moving boundary profile, we can compute further from (11) and (21) that

$$s(t) = b\exp\left[\varepsilon a t - \varepsilon\sum_{n=1}^{4}\frac{2(-1)^n(f_n n\pi - 2a)}{3\varepsilon a - 2(n\pi)^2}\left(e^{\left(3\varepsilon a - 2(n\pi)^2\right)\frac{t}{2}} - 1\right) + \mathcal{O}(\varepsilon^2)\right].$$

We still have to transform $s(t)$ back to the original variable $S(\tau)$. To do so, we write $s(t)$ in the following form:

$$s(t) = be^{\varepsilon a t}I(\varepsilon,t), \tag{22}$$

where

$$I(t) = \exp\left(-\varepsilon\sum_{n=1}^{4}\frac{2(-1)^n(f_n n\pi - 2a)}{3\varepsilon a - 2(n\pi)^2}\left(e^{\left(3\varepsilon a - 2(n\pi)^2\right)\frac{t}{2}} - 1\right) + \mathcal{O}(\varepsilon^2)\right).$$

We can expand I in a Taylor series around $\varepsilon = 0$, yielding

$$I(\varepsilon, t) = 1 + \varepsilon \sum_{n=1}^{4} \frac{(-1)^n}{(n\pi)^2}(f_n n\pi - 2a)(1 - e^{-(n\pi)^2 t}) + \mathcal{O}(\varepsilon^2),$$

which implies that

$$s(t) = be^{\varepsilon a t} + \mathcal{O}(\varepsilon).$$

If we take only the first term in the expansion for u, that is $N = 1$, then we can transform back to the original variable by writing $S(\tau) = s(t(\tau)) = be^{\varepsilon a t(\tau)}$ and by computing

$$\begin{aligned} t(\tau) &= \frac{\ln(S(\tau)/b)}{\varepsilon a} \Rightarrow \\ \frac{dt}{d\tau} = \frac{1}{S^2(\tau)} &= \frac{S'(\tau)}{\varepsilon a S(\tau)} \Rightarrow \\ S(\tau) &= \sqrt{b^2 + 2\varepsilon a \tau}. \end{aligned} \tag{23}$$

Alternatively, we can compute $S(\tau)$ implicitly. To do so, we compute first $s(t)$ for some values of t up to the Nth term. Then, for each t, we compute τ by using the inverse transformation

$$\tau(t) = \int_0^t s^2(\eta) d\eta. \tag{24}$$

For each τ obtained, we map it to the corresponding value of $s(t)$, yielding $S(\tau) = s(t(\tau))$. To see the influence of N on the approximations, we now choose a larger N. We take $N = 12$ to avoid length-2 Pythagorean chains because the smallest head of a length-2 chain is 13. For $N = 12$, the only triples are $(3, 4, 5)$ and $(6, 8, 10)$. We denote M_N as the set of natural numbers up to N excluding hypotenuse of any Pythagorean triple. In this case, we have $M_{12} = \{1, 2, 3, 4, 6, 7, 8, 9, 11, 12\}$. Thus, we have the following result for C_{0n}

$$C_{0n}(t_1) = \begin{cases} C_{05}(0)e^{\frac{3at_1}{2}} + C_{03}(0)C_{04}(0)\frac{125\pi}{9a}\left(e^{3at_1} - e^{\frac{3at_1}{2}}\right) + \cdots, & n = 5, \\ C_{010}(0)e^{\frac{3at_1}{2}} + C_{06}(0)C_{08}(0)\frac{250\pi}{9a}\left(e^{3at_1} - e^{\frac{3at_1}{2}}\right) + \cdots, & n = 10, \\ C_{0n}(0)e^{\frac{3at_1}{2}}, & n \in M_{12}. \end{cases}$$

We then calculate $s(t)$ up to 12 terms, yielding:

$$\begin{aligned} s(t) = b\exp\Bigg[\varepsilon a t - \varepsilon \Bigg(&\sum_{n=1}^{12} \frac{2(-1)^n(f_n n\pi - 2a)}{3\varepsilon a - 2(n\pi)^2}\left(e^{\left(3\varepsilon a - 2(n\pi)^2\right)\frac{t}{2}} - 1\right) \\ &- \frac{10(f_3 3\pi - 2a)(f_4 4\pi - 2a)}{12\pi(3\varepsilon a - 50\pi^2)}\left(e^{\left(3\varepsilon a - 50\pi^2\right)\frac{t}{2}} - 1\right) \\ &- \frac{20(f_6 6\pi - 2a)(f_8 8\pi - 2a)}{48\pi(3\varepsilon a - 200\pi^2)}\left(e^{\left(3\varepsilon a - 200\pi^2\right)\frac{t}{2}} - 1\right)\Bigg) + \mathcal{O}(\varepsilon^2)\Bigg]. \end{aligned}$$

For higher values of N, we still can compute and approximate the solution in the original variable $S(\tau)$ explicitly or implicitly by using the procedure as explained before. If we compare the approximation where $N = 12$ with the one where $N = 4$, then it turns out that the approximations are close to each other (see also Fig. 3). For that reason, we will use $N = 4$ in Section 5 of this paper for computing interfaces.

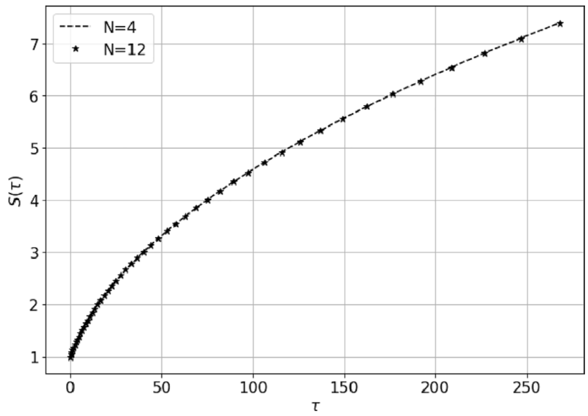

Fig. 3. Comparison of the approximations of the interface $S(\tau)$ for $N = 4$ and for $N = 12$.

4.4. Exact solution

To see how accurate the approximations are (which are constructed in the previous subsection), we will now compute an exact solution of a special Stefan problem with $h(t) = a$, where a is a constant. The method to be used is the similarity method. So, we start again with problem (2a)–(2e), where $H(T) = a$. By using the similarity method we look for solutions in the form:

$$U(X,\tau) = y(z), \quad z = \frac{X}{\sqrt{\tau}}.$$

By substituting this transformation into the problem (2a)–(2e), one obtains an initial value problem that can be solved directly, yielding

$$y(z) = \varepsilon a \left(1 - \frac{\operatorname{erf}\left(\frac{z}{2}\right)}{\operatorname{erf}(\alpha)}\right). \tag{25}$$

From (25), the moving interface $S(\tau)$ can readily be obtained, yielding

$$S(\tau) = 2\alpha\sqrt{\tau}, \tag{26}$$

where α is a constant which can be obtained by solving

$$\varepsilon a = \sqrt{\pi}\operatorname{erf}(\alpha)\exp(\alpha^2)\alpha. \tag{27}$$

Eq. (27) cannot be solved analytically for α, but has to be solved numerically. In terms of u, the solution is given by

$$U(X,\tau) = \varepsilon a \left(1 - \frac{\operatorname{erf}\left(\frac{X}{2\sqrt{\tau}}\right)}{\operatorname{erf}(\alpha)}\right). \tag{28}$$

Observe that this solution is a very special solution and does not involve initial condition. Setting $\tau = 0$ yields $S = 0$, which means the domain of the problem, i.e. $[0, S]$ is only a point set. This implies that the similarity method only gives the exact solution of the Stefan problem for which initially no water phase is present.

4.5. Comparing the results

In this subsection, we compare the approximation of the solution as obtained by using a multiple-time scales perturbation method with exact solution as obtained by using the similarity method.

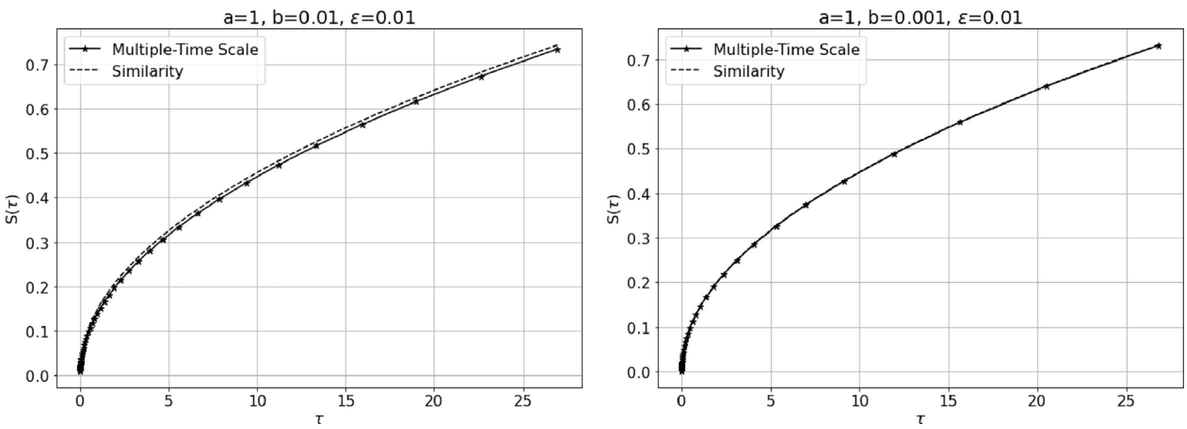

Fig. 4. Moving boundary profile for small values of b.

4.5.1. Negligible initial condition

The similarity solution describes the case with $b = 0$. However, we cannot take $b = 0$ in the multiple time scales approach, as this will cause the moving interface solution to vanish (see Eq. (11)). One way to manage this is by taking very small values for b. In this way, initially the temperature inside the domain is still very low and the amount of melted water is very small. So, in this way, the initial condition can be assumed to be negligible.

We take $a = 1$. As shown in Fig. 4, both solutions are getting close to each other as b decreases. When b is very small, i.e. $b = 0.001$, the two solutions coincide.

4.5.2. Stationary initial condition

In this subsection, we will use as initial condition, the ones which follow from the exact similarity solution for a given time. Consider the exact solution (28), and as an initial condition, we choose:

$$f(x) = a\left(1 - \frac{\mathrm{erf}(\alpha x)}{\mathrm{erf}(\alpha)}\right). \tag{29}$$

Then, the solution is a stationary solution for all time. Computing the Fourier coefficient f_n of this initial condition, yields

$$f_n = \frac{a}{\pi n}\left[2 + \frac{e^{-\frac{(n\pi)^2}{4\alpha^2}}}{\mathrm{erf}(\alpha)}\left(\mathrm{erf}\left(\alpha + \frac{in\pi}{2\alpha}\right) + \mathrm{erf}\left(\alpha - \frac{in\pi}{2\alpha}\right)\right)\right].$$

Now it should be observed that $\lim_{\alpha\to 0} f_n = \frac{2a}{\pi n}$, and from (27), it follows that $\lim_{\varepsilon\to 0}\alpha(\varepsilon) = 0$. This implies that smaller values of ε lead to f_n tending to $\frac{2a}{n\pi}$. This limiting value for f_n is important as it will cancel terms in the summations in the solution for u and s (see Eq. (21) and (22)). Thus, for small enough ε, the solution of $S(\tau)$ can be simplified to (23). We then use these f_n's to compute $s(t)$ by using the multiple-time scale perturbation method.

To compare the two solutions in this case, we must first determine the initial condition in the original variable S. For a given value of b, we can compute the time $\tau_0 = (b/2\alpha)^2$ for which $S(\tau_0) = b$. Shifting the time coordinate, we can determine a new moving boundary profile from the exact solution as

$$S(\tau) = 2\alpha\sqrt{\left(\frac{b}{2\alpha}\right)^2 + \tau} = \sqrt{b^2 + 4\alpha^2\tau}, \tag{30}$$

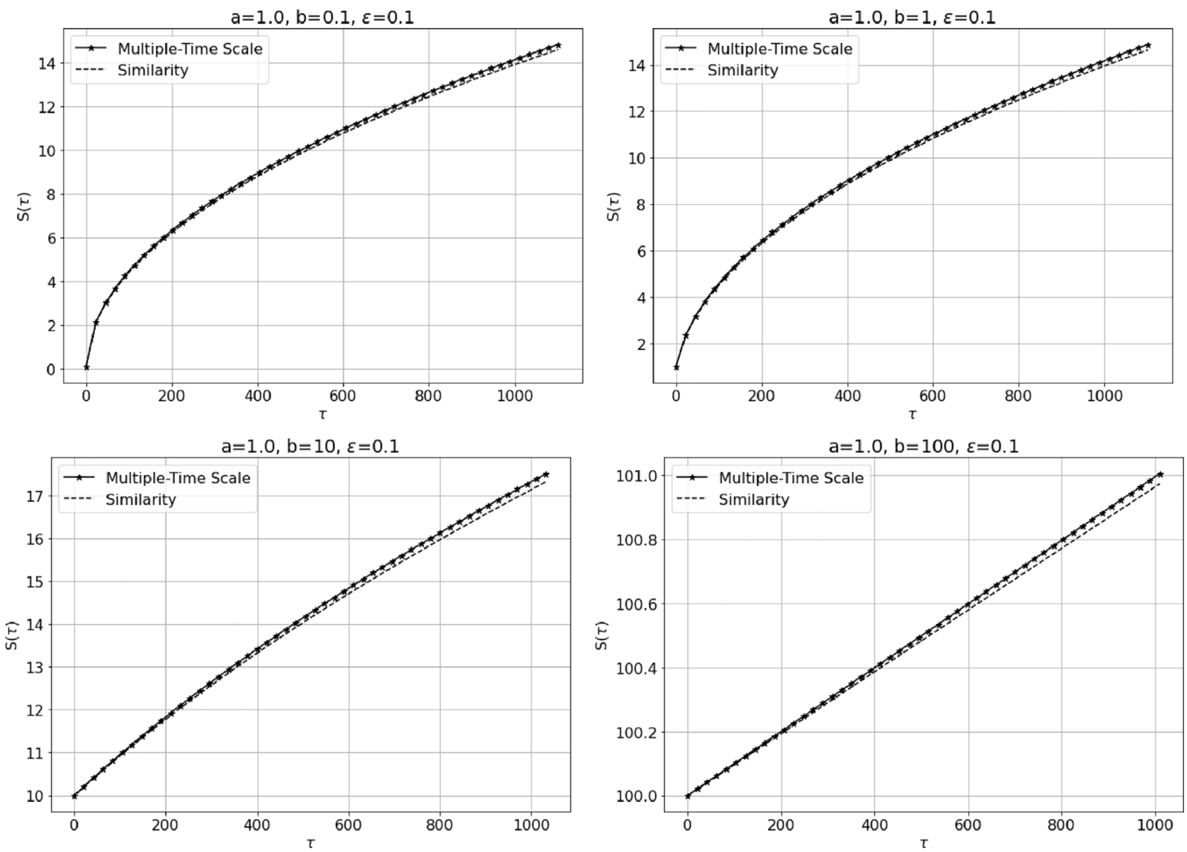

Fig. 5. Moving interface profile for the stationary exact solution and its approximation for different values of b.

so that "$S(0) = b$" as we intended. This form is similar to the one we obtain from the multiple-time scale method, i.e., from (23). Furthermore, it follows from the Taylor series around $\alpha = 0$ of the right-hand side of Eq. (27) that

$$\varepsilon a = 2\alpha^2 + \mathcal{O}(\alpha^4).$$

And this implies that the multiple-time scales solution of $S(\tau)$ in (23) can be written as

$$S(\tau) = \sqrt{b^2 + 2\varepsilon a\tau} \approx \sqrt{b^2 + 4\alpha^2\tau},$$

which coincides with the exact solution $S(\tau)$, given by (30). In this way, we indicated that the approximations obtained by using the multiple-time scales method and the exact solution remain close to each other for large times. The exact solution and its approximation are plotted in Fig. 5. The plot also shows that the exact solutions and its approximation remain very close to each other (not only for large times τ, but also for relatively large values of b).

5. Time varying temperature inputs at the fixed endpoint

5.1. The case $h(t)$ is periodic

Let us consider the more general case, where the temperature at $x = 0$ is T-periodic and positive definite. We assume that T is $\mathcal{O}(1)$. We can expand $h(t)$ in its Fourier series $a + \sum_{n=1}^{\infty} (A_n \sin(\kappa_n t) + B_n \cos(\kappa_n t))$, where $\kappa_n = \frac{2n\pi}{T}$ for given constants a, A_n, and B_n. The solution for u_{0n} now follows from (6) and is given by

$$u_{0n}(t_0, t_1) = Q_n(t_1)e^{-(n\pi)^2 t_0} - R_n(t_0), \tag{31}$$

where $Q_n(t_1) = C_{0n}(t_1) + R_n(0)$, and

$$R_n(t_0) = \sum_{m=1}^{\infty} \frac{2\kappa_m \left[(A_m(n\pi)^2 + B\kappa_m)\cos(\kappa_m t_0) + (A_m\kappa_m - B_m(n\pi)^2)\sin(\kappa_m t_0)\right]}{n\pi((n\pi)^4 + \kappa_m^2)}.$$

Computing the next order term in the approximation of the solution leads to similar results (see the formula after Eq. (14)) as in the case of constant temperature at the boundary, i.e.,

$$\int_0^{t_0} e^{(n\pi)^2\eta} H_{1n}(\eta, t_1)d\eta = \left[Q_n' - \frac{3aQ_n}{2} + 2\sum_{p\neq n} p\pi(-1)^p Q_{\sqrt{n^2-p^2}} Q_p K_{\sqrt{n^2-p^2}n}\right] t_0 + n.s.t.,$$

where $n.s.t$ stands for "non-secular terms". To remove the secular terms in the above equation, we need to consider again the Pythagorean triples as discussed before. Obtaining the solution in C_{0n} explicitly is too complicated because of the existence of Pythagorean triples. We apply again the truncation method and consider the case without Pythagorean triples. We derive that $Q_n(t_1) = Q_{0n}(0)e^{\frac{3at_1}{2}}$, where

$$Q_{0n}(0) = \left[f_n - \frac{2}{n\pi}\left(a + \sum_{m=1}^{\infty}\left(B_m + \kappa_m \frac{A_m(n\pi)^2 + B_m\kappa_m}{((n\pi)^4 + \kappa_m^2)}\right)\right)\right].$$

For the moving boundary profile, we have a similar form as for the constant case, i.e. $s(t) = be^{\varepsilon at}I(\varepsilon, t)$, where

$$I(\varepsilon, t) = \exp\left[-2\varepsilon\sum_{n=1}^{4}\left[\frac{Q_n(0)\left(e^{\left(\frac{3\varepsilon a}{2} - (n\pi)^2\right)t} - 1\right)}{3\varepsilon a - 2(n\pi)^2} n\pi(-1)^n + J_n(t)\right] + \mathcal{O}(\varepsilon^2)\right],$$

and

$$J_n(t) = \sum_{m=1}^{\infty} \frac{(A_m(n\pi)^2 + B\kappa_m)\sin(\kappa_m t) - (A_m\kappa_m - B_m(n\pi)^2)(\cos(\kappa_m t) - 1)}{(n\pi)^4 + \kappa_m^2}(-1)^n + \frac{A_n(\cos(\kappa_n t) - 1) - B_n\sin(\kappa_n t)}{2\kappa_n}.$$

This result is actually almost similar to the case of the constant boundary temperature, except for the additional periodic terms J_n. We now expand I around $\varepsilon = 0$ to obtain

$$I(\varepsilon, t) = 1 + \varepsilon\sum_{n=1}^{\infty}\left(\frac{Q_n(0)(-1)^n(1 - e^{-(n\pi)^2 t})}{n\pi} + J_n(t)\right) + \mathcal{O}(\varepsilon^2).$$

When we assume that A_n and B_n are relatively small compared to a, then we can neglect J_n and obtain the same result as for the constant temperature boundary case, i.e., $s(t) = be^{\varepsilon at} + \mathcal{O}(\varepsilon)$. We can see this case also as a small wiggle around constant temperature a at the boundary. The movement of the interface $s(t)$ is dominantly influenced by the average boundary temperature, which is the constant a, giving us a similar profile as for the constant temperature case.

5.2. The case $h(t)$ is periodic with a relatively large amplitude

In this subsection, a more specific case for a periodic temperature profile at the fixed endpoint is considered. In the last subsection, we see that the moving boundary profile tends to be the same as for

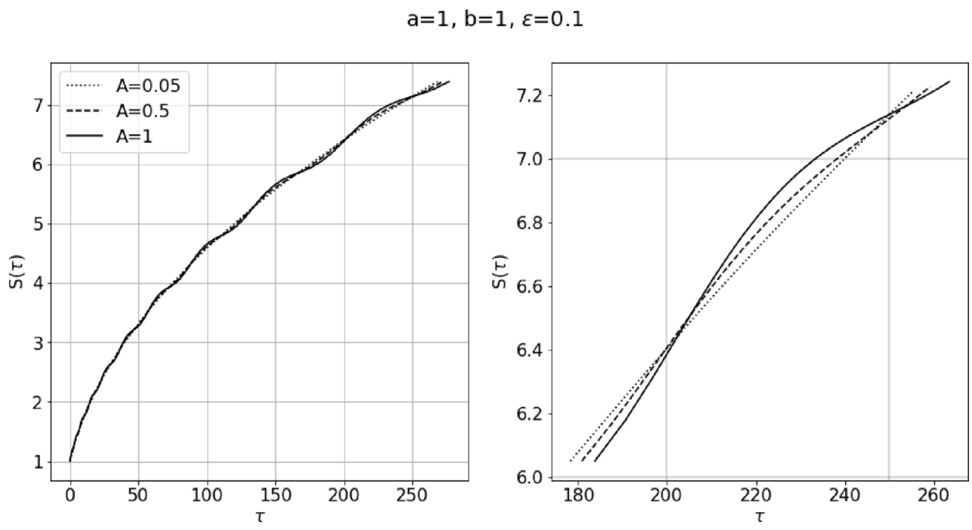

Fig. 6. Position of the moving boundary in case of a periodic temperature at the fixed endpoint for different values of A. The left figure is the position from initial time and the right one is a zoom-in at the τ-interval $[200, 250]$.

the constant case when the periodic part can be ignored. Let us now assume that we have large amplitudes A_n or B_n, so that the periodic part might significantly influence the interface movement. We consider a simple form for the boundary temperature profile: $h(t) = a + A\sin(\pi t)$ where A is assumed to be large but $|A| < a$ (in order to avoid additional occurrences of water–ice interfaces originating at $x = 0$ when $|A| > a$). The solution $s(t)$ is as before approximated by:

$$s(t) = \exp\left[-2\varepsilon \sum_{n=1}^{4} (-1)^n \left(\frac{Q_n(0)\left(e^{\left(\frac{3\varepsilon a}{2} - (n\pi)^2\right)t} - 1\right) n\pi}{3\varepsilon a - 2(n\pi)^2} + A\left(\frac{n^2\pi\sin(\pi t) - \cos(\pi t) + 1}{\pi(n^4\pi^2 + 1)}\right)\right) + \frac{A\varepsilon(\cos(\pi t) - 1)}{\pi} + \varepsilon a t + \mathcal{O}(\varepsilon^2)\right],$$

and can be written as follows

$$s(t) = e^{\varepsilon\left(at + A\frac{(\cos(\pi t) - 1)}{\pi}\right)} I(\varepsilon, t),$$

where

$$I(\varepsilon, t) = \exp\left[-2\varepsilon \sum_{n=1}^{4} (-1)^n \left(\frac{Q_n(0)\left(e^{\left(\frac{3\varepsilon a}{2} - (n\pi)^2\right)t} - 1\right) n\pi}{3\varepsilon a - 2(n\pi)^2} + 2A\frac{n^2\pi\sin(\pi t) - \cos(\pi t) + 1}{\pi(n^4\pi^2 + 1)}\right)\right].$$

Expanding I in ε yields

$$s(t) = e^{\varepsilon\left(at + A\frac{(\cos(\pi t) - 1)}{\pi}\right)} + \mathcal{O}(\varepsilon).$$

The results for different values of A are given in Fig. 6. We can see that for small A, the profile tends to behave as in the constant case for $h(t)$. In the case of larger values of A, the interface profile has a small wiggle, showing that the speed of the interface movement varies periodically. If we increase A, then the wiggle will get larger.

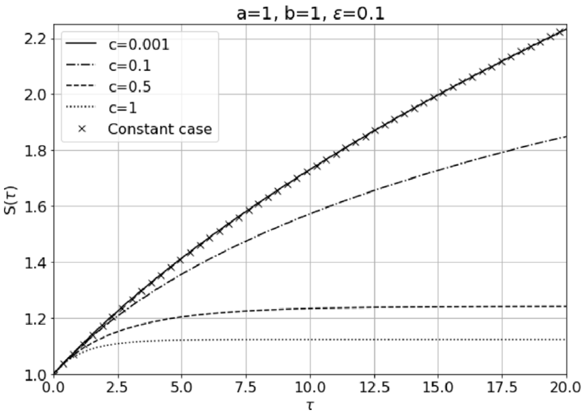

Fig. 7. The moving boundary profile in case of a decaying temperature at the fixed endpoint for different values of the decaying rate c.

5.3. The case $h(t)$ is decaying in time

Let us consider the case that $h(t)$ is exponentially decaying, i.e., $h(t) = ae^{-ct}$, where a and c are positive constants. The parameter c determines the decaying rate. The solution u_{0n} now becomes

$$u_{0n}(t_0, t_1) = C_{0n}(t_1)e^{-(n\pi)^2 t_0} + \frac{2ac(e^{-ct_0} - e^{-(n\pi)^2 t_0})}{n\pi((n\pi)^2 - c)}.$$

We can rewrite this solution for u_{0n} in the form as in Eq. (31), but with a different R_n:

$$R_n(t_0) = -\frac{2ace^{-ct_0}}{n\pi((n\pi)^2 - c)}.$$

By computing the next order term in the approximation of the solution, we obtain

$$\int_0^{t_0} e^{(n\pi)^2\eta} H_{1n}(\eta, t_1)d\eta = \left[Q'_n + 2\sum_{p\neq n} p\pi(-1)^p Q_{\sqrt{n^2-p^2}} Q_p K_{\sqrt{n^2-p^2}n}\right] t_0 + n.s.t..$$

To avoid secular terms, it follows as before that $Q'_n = 0$ for $n < 5$, and so, for $n < 5$:

$$C_{0n}(t_1) = C_{0n}(0) = \left(f_n - \frac{2a}{n\pi}\right).$$

When we use again the truncation method, and only take into account the first four terms in the summation, it follows that the position $s(t)$ of the moving boundary is given by:

$$s(t) = b\exp\left[\varepsilon \sum_{n=1}^{4} \frac{(-1)^n}{n\pi}\left(f_n - \frac{2a((n\pi)^2)}{n\pi((n\pi)^2 - c)}\right)(e^{-(n\pi)^2 t} - 1)\right.$$
$$\left. -\frac{\varepsilon a}{c}\left(1 - \sum_{n=1}^{4} \frac{2c(-1)^n}{((n\pi)^2 - c)}\right)(e^{-ct} - 1) + \mathcal{O}(\varepsilon^2)\right].$$

As before $S(\tau)$ can be implicitly computed from $s(t)$, and the results for different values of c are shown in Fig. 7. We can see that for smaller values of c, the profile tends to approach the profile as in the case for constant $h(t)$.

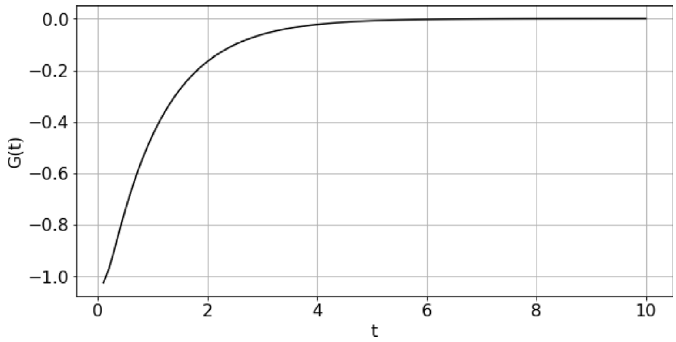

Fig. 8. Plot of $G(t)$ in time ($c = 1$).

For large enough values of c, we can already see in Fig. 7 that for some point in time, the interface becomes more or less steady. To study this behavior, we take the derivative of s with respect to t. For ease of computation, we denote first

$$D_n = \frac{(-1)^n}{n\pi}\left(f_n - \frac{2a((n\pi)^2)}{n\pi((n\pi)^2 - c)}\right), \qquad \text{and} \qquad E = \frac{\varepsilon a}{c}\left(1 - \sum_{n=1}^{4}\frac{2c(-1)^n}{((n\pi)^2 - c)}\right),$$

so that we can write

$$s(t) = b\exp\left(\varepsilon\sum_{n=1}^{4} D_n(e^{-(n\pi)^2 t} - 1) - \varepsilon E(e^{-ct} - 1)\right).$$

Then, we compute

$$\frac{ds}{dt} = -\varepsilon s(t)\left(\sum_{n=1}^{4}(n\pi)^2 D_n e^{-(n\pi)^2 t} - cEe^{-ct}\right).$$

To find the time for which the interface almost stops moving, we set the terms inside the brackets (denote it as $G(t)$) to zero. However, if we plot $G(t)$ with respect to t (assuming that $f(x)$ represents the stationary solution), we obtain the following profile as shown in Fig. 8, which shows that $G(t)$ only asymptotically tends to zero for t tending to infinity. Alternatively, we can now solve $|G(t)| < \delta$ for some small tolerance value δ to get the time when the interface almost stops moving.

6. Conclusion

This work presents an approach to construct approximations of the solutions for the phase change heat transfer problem with small time-dependent Dirichlet boundary condition by using the multiple-time scales perturbation method. It is shown that the obtained approximations of the solutions agree well with the exact solutions for the cases where exact solutions are available. By using the multiple-time scales perturbation method, we successfully simulate and analyze the dynamics of the problem for different boundary conditions at the fixed endpoint. Examples with time-periodic temperatures and with decaying temperatures at the fixed endpoint have been treated in detail. The applicability of this method to the present problem opens possibilities for future research on more complicated Stefan problems.

Acknowledgments

A.F. Ihsan's research is supported by ITB post-graduate voucher scholarship, Indonesia. J.M Tuwankotta's research is supported by Riset P2MI FMIPA ITB 2022.

References

[1] A.D. Solomon, D.G. Wilson, V. Alexiades, An Approximate Solution to the Problem of Solidification of a Sphere of Supercooled Fluid, Oak Ridge National Laboratory, 1986.
[2] R.V. Seeniraj, T.K. Bose, One-dimensional phase-change problems with radiation-convection, J. Heat Mass Transfer ASME 104 (1982) 811–813.
[3] A.D. Solomon, V. Alexiades, D.G. Wilson, The Stefan problem with a convective boundary condition, Quart. Appl. Math. 40 (2) (1982) 203–217.
[4] A.D. Solomon, D.G. Wilson, V. Alexiades, A mushy zone model with an exact solution, Lett. Heat Mass Transfer 9 (2) (1982) 319–324.
[5] R. Bonnerot, P. Jamet, A conservative finite element method for one-dimensional Stefan problems with appearing and disappearing phases, J. Comput. Phys. 41 (2) (1981) 357–388.
[6] S.L. Mitchell, S. O'Brien, Asymptotic, numerical and approximate techniques for a free boundary problem arising in the diffusion of glassy polymers, Appl. Math. Comput. 219 (1) (2012) 376–388.
[7] S.L. Mitchell, S. O'Brien, Asymptotic and numerical solutions of a free boundary problem for the sorption of a finite amount of solvent into a glassy polymer, SIAM J. Appl. Math. 74 (3) (2014) 697–723.
[8] F.J. Vermolen, C. Vuik, A mathematical model for the dissolution of particles in multi-component alloys, J. Comput. Appl. Math. 126 (2000) 233–254.
[9] J. Crank, Free and Moving Boundary Problems, Oxford University Press, Oxford, 1984.
[10] S. Gupta, The classical Stefan problem, Elsevier, 2003.
[11] A.C. Briozzo, D.A. Tarzia, Existence, uniqueness, and an explicit solution for a one-phase Stefan problem for a non-classical heat equation, Int. Ser. Numer. Mech. 154 (2006) 117–124.
[12] D.G. Wilson, Existence and uniqueness for similarity solutions of one dimensional multi-phase Stefan problems, SIAM J. Appl. Math. 35 (1) (1978) 135–147.
[13] J. Caldwell, Y.Y. Kwan, A brief review of several numerical methods for one-dimensional Stefan problems, Therm. Sci. 13 (2) (2009) 61–72.
[14] A.F. Ihsan, J.M. Tuwankotta, Godunov method for Stefan problems with Neumann and Robin type boundary condition using dimensionless enthalpy formulation, AIP Conf. Proc. 2296 (1) (2020) 020086, http://dx.doi.org/10.1063/5.0030769.
[15] R. Parambu, A. Awasthi, V. Vimal, N. Jha, A numerical implementation of higher-order time integration method for the transient heat conduction equation with a moving boundary based on boundary immobilization technique, AIP Conf. Proc. 2336 (030011) (2021).
[16] L. Qu, F. Ling, Numerical study of phase change problem with periodic boundary condition, Int. Conf. Adv. Mechatron. Syst. (6025004) (2011) 149–154.
[17] L. Qu, L. Xing, Z.Y. Yu, F. Ling, Numerical simulation of the melting problem of the boundary heat source changing with time, J. Eng. Therm. Energy Power 30 (5) (2015) 689–695.
[18] F.J. Vermolen, On similarity solutions and interface reactions for a vector-valued Stefan problem, Nonlinear Anal. 12 (2007) 268–288.
[19] J. Caldwell, Y.Y. Kwan, On the perturbation method for the Stefan problem with time-dependent boundary conditions, Int. J. Heat Mass Transfer 46 (2003) 1497–1501.
[20] F.I. Dragomirescu, K. Eisenschmidt, C. Rohde, B. Weigand, Perturbation solutions for the finite radially symmetric Stefan problem, Int. J. Therm. Sci. 104 (2016) 386–395.
[21] C.-L. Huang, Y.-P. Shih, Perturbation solution for planar solidification of a saturated liquid with convection at the wall, Int. J. Heat Mass Transfer 18 (1975) 1481–1483.
[22] H. Osman, S.M.M. Rasid, K.A. Arshad, S. Ahmad, Perturbation methods for one-phase Stefan problems involving homogeneous materials, World Appl. Sci. J. 17 (2012) 44–48.
[23] M. Parhizi, A. Jain, Solution of the phase change Stefan problem with time-dependent heat flux using perturbation method, J. Heat Mass Transfer 141 (2019) 1–5.
[24] J.S. Vrentas, D. Shin, Perturbation solutions of spherical moving boundary problems, Chem. Eng. Sci. 35 (1980) 1687–1696.
[25] Z.T. Yu, L.W. Fan, Y.C. Hu, K.F. Cen, Perturbation solution to heat conduction in melting or solidification with heat generation, J. Heat Mass Transfer 46 (2010) 479–483, http://dx.doi.org/10.1007/s00231-010-0596-4.
[26] A.F. Ihsan, W.T. van Horssen, J.M. Tuwankotta, On a multiple time-scales perturbation approach for a Stefan problem with a time-dependent heat flux at the boundary, Nonlinear Dyn. (2022) http://dx.doi.org/10.1007/s11071-022-07734-7.
[27] M.H. Holmes, Introduction to perturbation techniques, second ed., Springer, NewYork, 2010.
[28] J. Kevorkian, J.D. Cole, Multiple scale and singular perturbation methods, in: Applied Mathematical Sciences, Vol. 114, Springer-Verlag, 1996.
[29] A.H. Nayfeh, Introduction to perturbation techniques, John Wiley & Sons, Canada, 1993.